Scripta Materialia 133 (2017) 14–18

Contents lists available at ScienceDirect

Scripta Materialia

journal homepage: www.elsevier.com/locate/scriptamat

Regular article

A new strategy to fabricate nanoporous iron-based metallic glasses: Selective phase tailoring of amorphous-nanocrystalline composite alloys through electrochemical dissolution

Yu Jin [a], Ran Li [a,*], Hongjie Xu [a], Xiao-Bo Chen [b], Tao Zhang [a,*]

[a] Key Laboratory of Aerospace Materials and Performance (Ministry of Education), School of Materials Science and Engineering, Beihang University, Beijing 100191, China
[b] Department of Materials Science and Engineering, Monash University, Clayton, Victoria 3800, Australia

ARTICLE INFO

Article history:
Received 2 December 2016
Received in revised form 26 January 2017
Accepted 26 January 2017
Available online xxxx

Keywords:
Iron alloys
Amorphous materials
Nanocrystalline metal
Selective dissolution
Rapid solidification

ABSTRACT

A feasible strategy was developed to fabricate nanoporous iron-based metallic glasses (npFe-MGs) by selective dissolution of the electrochemically active α-Fe nanocrystalline phase from Fe-Nb-B composite alloys. The yielded npFe-MGs exhibited a ligament size of ~75 nm and a pore size of ~120 nm. Morphology of the npFe-MGs (*i.e.* pore size and pore number) could be tailored by the selection of precursor alloys prepared by varying rapid solidification conditions. Such a selective phase-tailoring approach provides new insights to the preparation of metallic glasses with promising nanoporous structure to satisfy a variety of engineering requirements, *e.g.* catalysis, microwave absorption, capacitor, *etc.*

Nanoporous metals with high surface area, low density and tunable microstructure have been studied intensively. Various nanoporous metals (especially noble ones), such as platinum (Pt), palladium (Pd), gold (Au), silver (Ag), nickel (Ni) and copper (Cu), have been fabricated through dealloying techniques for a broad range of applications, including catalysts, sensors, fuel cells, plasmonics, *etc.* [1–7]. Iron (Fe)-based alloys with nanostructure outperform these noble metal counterparts greatly owing to their high economic effectiveness and chemical activity [8–10]. It is well recognized that Fe-based nanoparticles and nanofilms are promising function materials, which is attributed to their unique magnetic properties (*e.g.* superparamagnetism) and specific catalytic activity (*e.g.* strong catalytic selectivity in regards to Fischer-Tropsch synthesis) [8,10]. However, compared to nanoporous noble metals, few studies have focused on the development of nanoporous Fe or Fe-based alloys by means of dealloying processes due to their high electrochemical activity [11].

Besides dealloying, selective electrochemical dissolution of active phase(s) from dual- and multi-phase alloys is a promising way to yield nanoporous materials, which can impose delicate controls over their geometrical features, such as size of ligaments and pores, through the selection of precursor alloys with appropriate compositions [12–15]. For instance, through selectively dissolved from two-phase metal-phosphides ribbons, metal phosphides with nanoporous structure were fabricated with controlled pore sizes varying from 30 to 300 nm by means of changing the cooling rate of precursors [12]. In addition, nanoporous Ti-based metallic glasses were synthesized by preferential dissolution of the active ingredients (*i.e.* yttrium (Y) and aluminum (Al)) from a two-phase $Y_{20}Ti_{36}Al_{24}Co_{20}$ metallic glass [14].It is of significance for fabricating Fe-based alloys with a controlled growth of nanostructure through selective electrochemical dissolution.

Fe-based alloys containing discrete phases (*e.g.* α-Fe nanocrystals embedded in amorphous Fe matrix) have been intensively investigated to employ their excellent soft magnetic properties for highly efficient soft magnetic transformers (especially for mediate- and high-frequency), anti-theft labels, *etc.* [16,17]. These composite alloys could be ideal precursors to prepare Fe-based metallic glasses with desired nanostructure. The α-Fe nanocrystals exhibit a higher electrochemical activity than their amorphous counterpart [18], which provides a solid paradigm to selectively eliminate the active Fe nanocrystals and retain the noble amorphous matrix.

Herein, nanoporous Fe-based metallic glasses (npFe-MGs) were fabricated by controlled electrochemical dissolution of α-Fe nanocrystals from Fe-Nb-B composite precursor alloys. To obtain proper microstructure, a number of compositions of the precursor alloys were explored as a function of Fe concentration from a good glass-former alloy of $Fe_{70}Nb_{10}B_{20}$ [19,20]. Electrochemical behavior of the precursor alloys was investigated by potentiodynamic polarization measurements to determine suitable conditions of selective phase tailoring. Moreover, morphology of the npFe-MGs was regulated through controls over the

* Corresponding authors.
E-mail addresses: liran@buaa.edu.cn (R. Li), zhangtao@buaa.edu.cn (T. Zhang).

http://dx.doi.org/10.1016/j.scriptamat.2017.01.029
1359-6462/

cooling rate of precursor ribbons with optimal alloy compositions during rapid solidification processes. The preparation strategy provides new insights for the preparation of nanoporous metallic glasses with desired structure and functionalities.

Ingots with a nominal composition of $Fe_{76+3x}Nb_{8-x}B_{16-2x}$ ($x = 0$, 1, 2 3, in atomic percentage) were prepared by arc-melting a mixture of pure Fe (99.5 wt.%), Nb (99.8 wt.%) and industry-grade pre-alloys Fe-B (21.0 wt% of B) under Ti gettered argon atmosphere. Precursor ribbons with a dimension of ~60 μm in thickness and 2 mm in width were fabricated by melt-spinning method at a constant linear speed of 20 m/s of Cu wheel (diameter: 25 cm) under argon atmosphere. Moreover, a set of linear speeds, saying 15, 20 and 30 m/s, respectively, were employed to the $Fe_{82}Nb_6B_{12}$ alloy to determine the impact of linear speed on the microstructure of the resulting ribbons. Corrosion behavior of $Fe_{82}Nb_6B_{12}$ was evaluated by means of potentiodynamic polarization measurements in a variety corrosive media, *i.e.* 0.5 M H_2SO_4, 0.3 M H_3PO_4, 0.1 M HCl, and 0.05 M NaCl aqueous solutions. Moreover, corrosion behavior of pure Fe (99.5 wt%) was also investigated in 0.3 M H_3PO_4 aqueous solution for comparison. An electrochemical workstation (Princeton VersaSTAT 3) and a three-electrode cell with saturated calomel electrode (SCE), a Pt plate counter electrode and a test sample were adopted to record potentiodynamic polarization curves with a potential sweep rate of 50 mV/min after 20 min's stabilization at open-circuit potential (OCP). In addition, $Fe_{82}Nb_6B_{12}$ ribbons were used as precursor materials to yield npFe-MGs using potentiostatic etching techniques at a constant electric potential (*i.e.* 0.0 V). When the etching process was finalized, the working electrodes, *i.e.* etched $Fe_{82}Nb_6B_{12}$ ribbons, were removed, rinsed with distilled water and absolute alcohol, and then dried in a vacuum chamber. Crystallographic composition of the nanocrystalline ribbons and the corroded samples was identified by X-ray diffraction (XRD) using a Dmax2200PC Rigaku X-ray diffractometer with Cu Kα radiation. Microstructure of the composite ribbons and the resulting npFe-MGs were examined by scanning electron microscopy (SEM, JEOL JSM-7500F), and transmission electron microscopy (TEM, JEM-2100F) operated at 200 keV equipped with an energy-dispersive X-ray analyzer (EDX).

Fig. 1(a) illustrates XRD patterns of $Fe_{76+3x}Nb_{8-x}B_{16-2x}$ ($x = 0$, 1, 2 and 3) composite ribbons fabricated by melt spinning at a constant linear speed rate of 20 m/s. XRD pattern of $Fe_{76}Nb_8B_{16}$ ($x = 0$) exhibits glassy structural characteristics with evident wide diffraction hump whilst without any crystalline features. The increase in the mass of added Fe from 79% to 85% (*i.e.* x varies from 1 to 3) leads to a gradual increment in the intensity of diffraction peaks of α-Fe phase, indicating a profound inhibition on the glass-forming ability of the precursor alloys. The unique broad diffraction hump of amorphous phases remains apparent in the samples with less addition of Fe ($x = 1$ and 2), demonstrating the formation of the amorphous-nanocrystalline composite structure, *i.e.* metallic glass matrix and α-Fe precipitate phase, as anticipated. Microalloying of Fe-based alloys with Nb and B plays a key role in stabilizing amorphous structure and suppressing the growth kinetics of nanocrystals [21]. As such, it is hypothesized that size and proportion of α-Fe crystalline phases could be well regulated through the selection of precursor alloys with appropriate chemical composition. To validate such hypothesis, Fe-based ribbons with a composition of $Fe_{82}Nb_6B_{12}$ (*i.e.* $x = 2$) were employed as a representative precursor alloy according to its characteristic XRD pattern containing both amorphous and crystalline identities.

TEM micrographs and selected area electron diffraction (SAED) pattern were employed to reveal the structural features of as-spun $Fe_{82}Nb_6B_{12}$ specimens collected from surface and center regions of the bulk material (Fig. 1(b)–(e)). The particle size and its distribution of the crystalline α-Fe precipitates demonstrate a strong region-dependent nature. In terms of surface region, grains (bright phases) with a diameter of approximate 120 nm are present in the net-like matrix (dark phases) with a ligament size varying between 20 and 240 nm (Fig. 1(b)). The inset SAED pattern (Fig. 1(b)) confirms the existence of

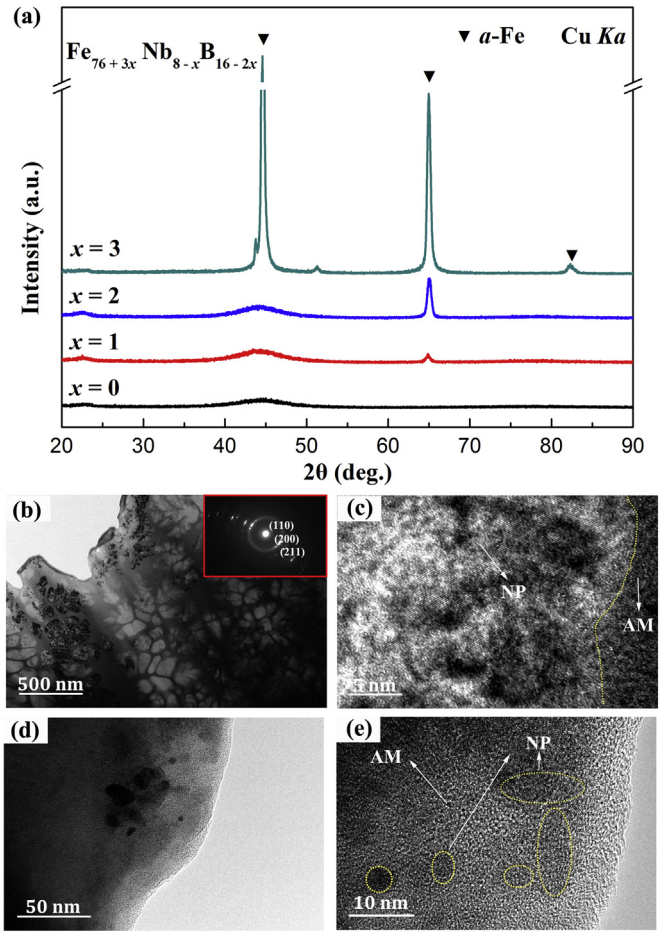

Fig. 1. (a) XRD patterns of as-spun $Fe_{76+3x}Nb_{8-x}B_{16-2x}$ ($x = 0, 1, 2, 3$) ribbons. TEM micrographs of as-spun $Fe_{82}Nb_6B_{12}$ ribbons in surface region: (b) bright field image (SAED pattern as inset) and (c) local HRTEM image. TEM micrographs of as-spun $Fe_{82}Nb_6B_{12}$ ribbons in center region: (d) bright field image and (e) HRTEM image. (AM: amorphous matrix, NP: nanocrystalline phase).

both amorphous phases (broad diffraction rings) and nanocrystalline α-Fe phases [22,23], which can be further convinced with a HRTEM micrograph (Fig. 1(c)). Regarding center area, on the contrary, no such a network structure exists in the bright-field TEM image (Fig. 1(d)). α-Fe nanoparticles with a smaller mean grain size of 5 ± 3 nm were embedded sparsely in the amorphous matrix (Fig. 1(d) and (e)). Such a region-dependent morphology of the α-Fe nanocrystalline phases in the $Fe_{82}Nb_6B_{12}$ ribbons is related to surface crystallization, which is attributed to diffusion and stress relaxation, or a local variation in surface composition during cooling [24]. Moreover, oxygen absorption on surface could restrain the glass-formation ability whilst accelerate the growth of α-Fe. As such, $Fe_{82}Nb_6B_{12}$ amorphous-nanocrystalline ribbons are an ideal precursor material to prepare npFe-MGs.

Corrosion behavior of $Fe_{82}Nb_6B_{12}$ composite alloy ribbons and pure Fe was monitored in 0.3 M H_3PO_4 aqueous solution at 298 K through electrochemical potentiodynamic polarization measurements (Fig. 2(a)). Pure Fe underwent a characteristic anodic dissolution with corrosion potential (−0.5 V *vs.* SCE) and a high estimated corrosion current density (1.5×10^{-4} A/cm^2). In contrast, $Fe_{82}Nb_6B_{12}$ composite alloy ribbons performed an active-passive transition, and exhibited a nobler corrosion potential (−0.43 V *vs.* SCE) and a lower corrosion current density (0.7×10^{-4} A/cm^2). Such an active-passive transition was initiated by the anodic dissolution of α-Fe phases and followed by a wide passivation region (as indicated in Fig. 2(a)), which is attributed to the formation of a passive film of Nb in the amorphous matrix. Similar corrosion behavior was reported with respective to a $Fe_{84.8}Zr_{3.4}Nb_{3.4}B_{7.4}Cu_1$